WOOD FIBRE MATERIALS ON HOT SOUNDING ROCKET STRUCTURES

Raphaela Günther[(1)], Oliver Hohn[(2)], Holger Unbehaun[(3)], Oliver Drescher[(4)], Hendrik Weihs[(5)]

(1) Technical University Dresden (TUD), Chair of Space Systems,
01307 Dresden, Germany, E-mail: raphaela_elisa.guenther@tu-dresden.de

(2) German Aerospace Center (DLR)/Cologne, Supersonic and Hypersonic Technologies
Department, 51147 Köln, Germany, E-mail: oliver.hohn@dlr.de

(3) Technical University Dresden (TUD), Professorship of Wood and Fibre Material Technology,
01307 Dresden, Germany, E-mail: holger.unbehaun@tu-dresden.de

(4) German Aerospace Center (DLR)/Oberpfaffenhofen, Mobile Rocket Base (MORABA),
82234 Weßling, Germany, E-mail: oliver.drescher@dlr.de

(5) German Aerospace Center (DLR)/Stuttgart, Institute for Structures and Design,
70569 Stuttgart, Germany, E-mail: hendrik.weihs@dlr.de

ABSTRACT

Throughout the history of aviation as well as space flight, wooden materials played a major role in the construction of primary as well as secondary structures. Being one of the first construction materials used in that field, it does not only offer low density and good relative strength properties, but also easy handling, simple production processes, low costs and last but not least a green, renewable resource. With its unique characteristics the worlds lightest and biggest aviation vehicles heavier than air were created.

Because of its relatively low thermal conductivity and good ablative behaviour wooden materials are taken into consideration for the use of hot structures such as the leading edges of sounding rocket stabilising fins. As a mandatory and thus flight critical structure of ballistic flying vehicles, fins need to be aerodynamically effective, lightweight, stiff and heat resistant on its foremost front end, where high temperatures may arise from fluid stagnation and friction. In order to gain a deeper understanding and assess the usability of modern wood fibre materials being appropriate in that field jointly, a cooperation with the Technische Universität Dresden (TUD) and the German Aerospace Center (DLR) has been established.

This paper describes the motivation of the research as well as the structural application with its functionality and boundary conditions. The choice of materials and its rationale for selection in combination with various screening test results are the core of this research. First impacts on the components´ design and an outlook for future research conclude this paper.

1. MOTIVATION

For almost eight decades sounding rockets represent an essential tool within the scientific community, especially in the fields of atmospheric physics, microgravity as well as hypersonic research. Therefore, the continuous development and optimisation of the respective flight vehicles as well as of systems and components are of major interest. Due to a low cost and high efficiency approach most of the vehicle's hardware cannot be reused after the flight. Only the most valuable scientific payload and payload support systems are commonly recovered and refurbished for re-flights, which are marked in red as an example for the VSB-30 in Fig. 1.
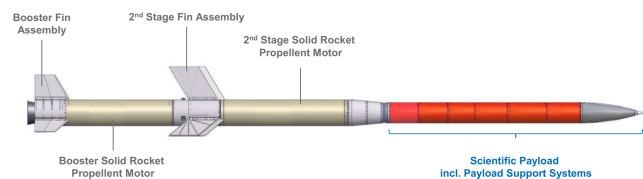

Figure 1: DLR Mobile Rocket Base (MORABA) VSB-30 two stage sounding rocket vehicle.

Under these circumstances, sustainability, especially of raw materials and manufacturing processes, becomes a stringent subject for the hardware that is lost after each vehicle operation.

Among these single-use components a variety of hot structures, such as the leading edges of the sounding rocket stabilising fins, can be found. As a mandatory and thus flight critical structure of ballistic flying vehicles, fins need to be aerodynamically effective, lightweight, stiff and heat resistant on its foremost front end, where high temperatures may arise from fluid stagnation and friction, see Fig. 2.
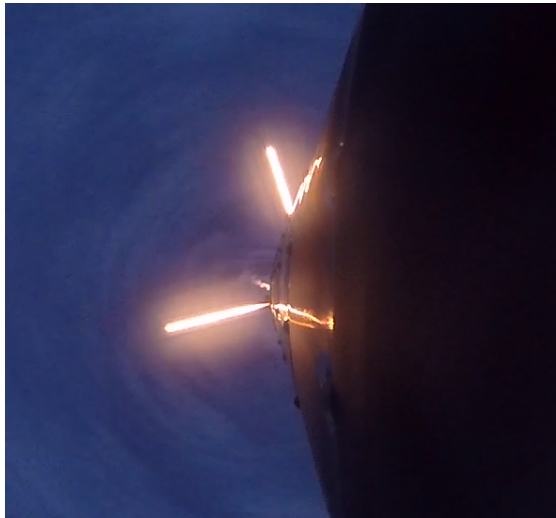

Figure 2: Thermal load on fin leading edges after 2ⁿᵈ stage burn of DLR MORABA sounding rocket vehicle.

A common solution to the leading edge being overheated can be the use of high temperature steel alloys, thermal protection system (TPS) layers or both in combination.

Figure 3: 2ⁿᵈ stage fin with steel sheet metal leading edge and ablative TPS recovered after VSB-30 flight operation.

The steel version needs to be lightweight, thus almost only sheet metal comes into consideration, which revealed to be critical in terms of thermal stress relief deformations effecting

the vehicle's flight mechanical performance. Layers of TPS around the leading edge need to be relatively thin and hence are rapidly "washed" away leaving the underlaying structure unprotected during later flight phases. Fig. 3 demonstrates both effects on a recovered 2ⁿᵈ stage fin after a typical VSB-30 flight where a combination of steel sheet metal leading edges with an ablative TPS was used.

As a consequence the DLR Institute of Structures and Design developed special phenolic glass fibre reinforced leading edges, which were introduced by DLR MORABA on all their thermally higher loaded fin assemblies. Even though this material serves the temperature load as well as the component's major specifications in a more appropriate way, its lack of lightweight design and sustainability as a "Green" material are immanent. However, sounding rockets are a very suitable test bed to verify component's material and structural concepts for all other launch systems. The application of "Green" materials to substitute ecological sensitive materials like phenolic cork or other critical thermal protection materials could help to enhance sustainability in space transportation significantly.

Based on the motivation described above, the following research question can be derived: *Which natural fibre-based material substitutes for sounding rocket fin leading edges are suitable to fulfil the thermal and mechanical requirements of a relevant mission of the DLR?*

Being thermally and mechanically one of the most challenging sounding rocket flights for DLR MORABA, the DLR STORT flight envelope has been taken as reference in order to explore the material candidate's boundaries. Solid wood and wood fibre materials are considered to identify preferred material variants based on natural fibres for fin leading edges. In this context, the already applied materials, a phenolic glass fibre reinforced material (comparative material 1) and a high temperature steel alloy (comparative material 2), are used for comparison.

2. PRELIMINARY TEST

The evaluation of a preliminary test serves as experimental basis. Test specimens made of the solid woods oak and mahogany as well as specimens of a preliminary test material 1 (PTM-1) based on carbon fibres and a preliminary test material 2 (PTM-2) based on a phenolic glass fibre reinforced composite were tested in the arc-heated wind tunnel L2K of the Institute of Aerodynamics and Flow Technology, Supersonic and Hypersonic Technologies (DLR). In addition to a mass and a cross-sectional area analysis, a microscopic analysis of micrographs took place.

A clear correlation between the anatomy of the wood species and their behaviour under thermal load can be seen. The large differences in pore size between early and late

wood as well as thicker wood strands cause a stronger degradation of the material. The orientation of the wood structure, especially the wood rays to the direction of load determines the burning behaviour. A uniform pore size, distribution of pores within the material, and a small difference between early and late wood, seem to prevent severe burning and support a more stable porous char layer.

3. REQUIREMENT ANALYSIS

The following general requirements for fin leading edges formulated by the DLR are considered:
- fail-safe at all times during the mission
- support aerodynamic loads of STORT mission in medium range and thermal loads in high range
- geometry and integrity maintenance over a long period of the flight

Further, optional requirements for fin leading edges from natural origin formulated by the DLR are defined:
- lower mass
- improvement in flight stability
- reduction of flutter behaviour
- reduction of the polar moment of inertia
- lower production costs
- reduction of requirements for post-flight NDI or structural health monitoring

Additional requirements set by TUD can be formulated for natural fibre-based fin leading edges, which must be met by all material types.
- high material strengths and densities to maintain structural integrity under mechanical and high thermal loads
- low thermal conductivity and high thermal resistance to prevent heat transfer throughout the fin structure and maintain geometry

4. MATERIAL SCREENING AND SELECTION

The materials to be tested should represent a wide range of material properties within their material type. Thus, the materials can be compared with each other in a more differentiated manner. As natural fibre-based materials, the materials solid wood, wood fibre materials and cork are selected. As solid woods, both softwoods and hardwoods are selected. In the case of wood fibre materials, industrial material is compared with material produced by the TUD. Among the possible tropical and native woods, domestic wood species are preferred for an application in a European sounding rocket, as they are readily available in Europe and reduce CO_2 emissions during harvesting, transport and logistics. Therefore, only regional, native wood species are considered in the material selection.

To identify most suited wood fibre materials for an application on fin leading edges, screening tests were carried out for the test material selection. The main stress on the leading edge of the fin is caused by thermal loads and the temperature resistance of the fin edge is a general requirement. Consequently, analyses to characterize thermal material properties form the basis for the selection of the material.

4.1 Thermogravimetric analysis (TGA)

Particular focus was placed on a thermogravimetric analysis (TGA), which provides information on the char yield and pyrolytic behaviour of a material by determining the change in mass of a test material as a function of temperature and time. In a first step, the pre-dried test specimens were heated from 25 °C to 105 °C in the TGA test device with a temperature increase of 15 K/min. Then, in a second step, the test specimens were heated from 105 °C to 1000 °C at 40 K/min. The measurement was carried out in a nitrogen atmosphere with a volume flow of 3.5 l/min.

The TGA is performed for the following materials, which are displayed before and after the analysis in Fig. 4:
- **I-WBM** (industrial wood based material, contains flame retardant)
- **TUD-WBM-0** (wood based material produced at TUD, 100 % wood fibre, flame retardant free)
- **TUD-WBM-1** (wood based material produced at TUD, 100 % wood fibre, contains bio-based flame retardant)
- **TUD-WBM-2** (wood based material produced at TUD, wood fibre and special natural fibre material, contains bio-based flame retardant)
- **Oak** (solid wood *Quercus petraea, Q. robur*)
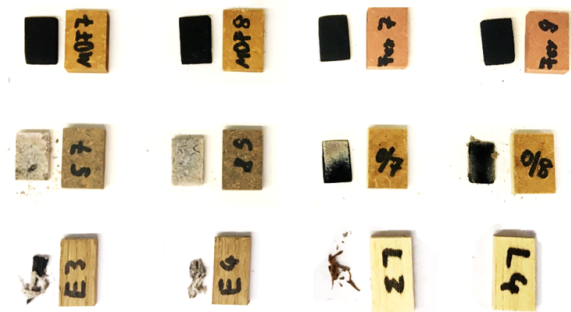- **Larch** (solid wood *Larix decidua, Larix* spp.)

Figure 4: Test specimens before (right) and after (left) TGA

A clear mass loss for all test specimens at 1000 °C can be seen in Fig. 5. The pre-drying results in a negligible mass loss due to the evaporation of water. The mass losses shown are exclusively caused by the ingredients of the test materials. The test specimens made of solid wood retain their mass up to a temperature of about 200 °C, after which it drops very steeply to less than 20 % (larch) and less than 30 % (oak). The TUD-WBM-0 test specimens have slightly higher residual mass percentages above 30 % compared to the solid wood test specimens. The I-WBM and TUD-WBM-1 test specimens still have 30 - 35 % of their original mass when they reach 1000 °C. The mass loss curves are similar and very close to each other. It is evident that the use of flame retardant has a positive effect on mass loss. As Fig. 4 shows, the surfaces of the I-WBM and TUD-WBM-1 samples are black and cracked or porous. The TUD-WBM-2 test specimens have the highest residual mass ratio of over 40 % and show light-coloured, mineral deposits on their surface. The higher residual masses of TUD-WBM-2 can be explained by the composition of the material. The natural salts, sandy residues and suspended matter contained in the special natural fibre material have high melting points (sodium chloride/ salt: $T_M \sim 801$ °C [1], quartz sand: $T_M \sim 1713$ °C [2]), which slow down the decomposition of the material and thus act as natural flame retardants. These components, which are not decomposed, form the light-coloured, mineral deposits on the test specimen surface that can be seen after the measurements. All wood fibre materials retain their material cohesion. The test specimens of the solid woods are very disjointed after the test and partially charred and ashen.
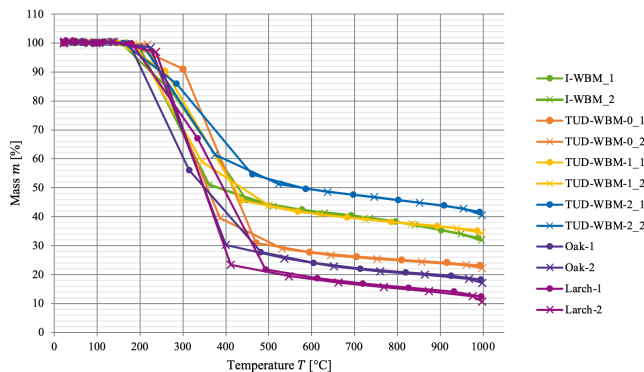

Figure 5: Test results of TGA

4.2 Thermal material characterisation

In addition, for the material screening the bulk density, thermal conductivity and specific heat capacity were determined for the wood based materials. The results and literature values for the remaining materials are shown in table 1.

Table 1: Properties of test materials

Material	Bulk density ρ [g/cm^3]	Thermal conductivity λ [W/mK]	Specific heat capacity c_p [J/kgK]
I-WBM	0.80	0.225	1446.0
TUD-WBM-1	0.87 [+]	0.353 (plane)	1467.7
TUD-WBM-2	0.89 [+]	0.252	1493.2
Oak	0.71 [3] 0.66[+]	0.166 [4]	-
Larch	0.60 [3] 0.55 [+]	0.114 [4]	-
Comparative Material 1	2.0 ± 0.1	0.4 ± 0.1	> 850
Comparative Material 2	7.9	15	500

[+] Measurements at TUD

The thermal conductivities of all wood fibre materials are less than half the thermal conductivities of the comparative materials 1 and 2. This means that the natural fibre-based materials insulate heat better and transfer less heat to the fin when used in fin leading edges. Compared with literature values of $\lambda = 0.18$ W/mK according to DIN EN ISO 10456 for wood fibre boards with bulk densities of 0.8 g/cm^3 [5], the analysed materials have higher thermal conductivities.

The values of the specific heat capacity of all analysed materials are very close to each other. The specific heat capacities of the wood fibre materials are more than twice (comparative material 1) or three times (comparative material 2) as large as those of previously used materials. This means that the natural fibre-based materials can store heat better or have a lower temperature rise in the material. For the use of these materials in fin leading edges, more heat would be required to heat the material compared to the fin leading edge materials used so far. Compared to literature values of $c_p = 1700$ W/mK according to DIN EN ISO 10456 for wood fibre boards with bulk densities of 0.8 g/cm^3 [5], the analysed materials have lower specific heat capacities.

4.3 Material selection

The thermal material properties verify the materials selected for the TGA very well. The test specimens for L2K of the selected materials are shown in Fig. 6.

For the solid woods, the softwood larch and the two hardwoods oak and birch were chosen. Two hardwoods and one softwood were selected because hardwoods have higher average strengths and bulk densities. Oak was selected as a ring-porous wood with a high bulk density of 0.71 g/cm^3 [6] and birch as a dispersed-porous wood due to its high elasto-mechanical properties. Larch, with a bulk density of

0.6 g/cm³ [6], has the highest bulk density of all European softwood species, making it the heaviest and hardest native softwood. Due to a deviating origin and regionality of the solid woods, the calculated density of oak for test specimens of the preliminary test ($\rho = 0.83$ g/cm³), for example, is higher than that of oak for the test specimens ($\rho = 0.66$ g/cm³).

For the wood based materials, an industrially produced fibre board material I-WBM was selected, which was developed for increased fire protection requirements in non-load-bearing interior applications in dry areas. In the context of the investigations, it represents an industrial comparative material. The TUD-WBM-1 and TUD-WBM-2 materials from TUD were also selected. For wood fibre materials they have high average bulk densities of 0.87 g/cm³ and 0.89 g/cm³.

Figure 6: Test specimen of selected material

5. TESTING

In the scope of testing, the test facility, the test conditions and test specimens are described below. Further, test results are presented.

5.1 Arc-heated wind tunnel L2K

The arc-heat wind tunnel facilities LBK of DLR Cologne are certified by ESA as a European key facility for testing and qualification of thermal protection systems. The LBK facilities consist of two nearly independent test legs, called L2K and L3K. The setup of the facilities is schematically plotted in Fig. 7. The two legs share a common system of vacuum pumps and exhaust gas cleaning as well as the low-pressure cooling cycle for the test chamber and the heat exchangers in the diffusors. Apart from this, the facilities can operate independently as each is equipped with their own power and gas supply, arc heater cooling systems and controls.
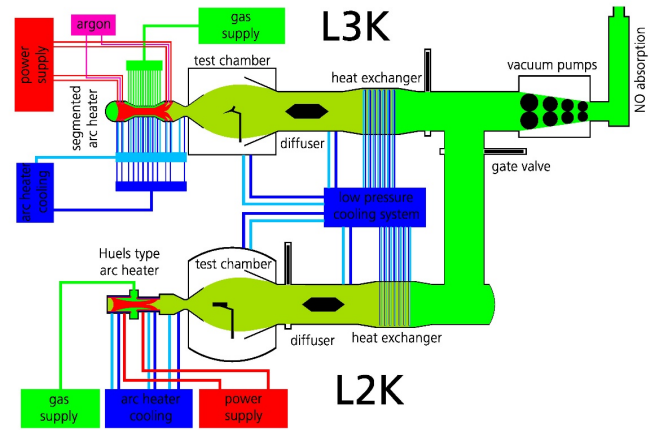

Figure 7: Schematic overview of the arc-heated wind tunnel facilities LBK

The L2K facility is equipped with a Huels-type arc heater for gas mass flow rates between 5 and 75 g/s. With a maximum power of 1.4 MW moderate specific enthalpies up to 10 MJ/kg are achieved at a gas mass flow rate of 50 g/s, which corresponds to a reservoir pressure of about 1500 hPa. As the working gases, air, nitrogen, argon or mixtures e.g. for Martian (CO_2/N_2) or Titan (N_2/CH_4) atmospheres can be used.

Hypersonic free stream velocities are provided by a convergent-divergent nozzle. The nozzle's expansion part is conical with a half angle of 12°. Different throat diameters from 14 mm to 29 mm are available and can be combined with nozzle exit diameters of 50 mm, 100 mm, and 200 mm. Accordingly, the facility setup can effectively be adapted to particular necessities of a certain test campaign. More detailed descriptions of the L2K facility are given by Gülhan et al. [7],[8],[9].

5.2 Test condition and test specimens

The test condition was chosen to represent the case of maximum total enthalpy encountered during the projected STORT flight trajectory which occurs at an altitude of approximately 41.5 km at a flight Mach number of 8.6. At this point the vehicle experiences a total enthalpy of about $h_0 = 4.048$ MJ/kg at a stagnation pressure of $p_s = 254$ hPa. With these values, the parameter

$$h_0 \cdot \sqrt{p_s} \sim 64.5$$

can be calculated as a reference value for the thermal load, when h_0 is entered in the unit MJ/kg and p_s in hPa.

This parameter can then be used as a similarity parameter for determining the wind tunnel conditions. Furthermore, it has to be considered that the flow in L2K is in thermal and chemical non-equilibrium with a rather high portion of atomic oxygen from dissociation in the arc-heater, when air is used as a test gas, whereas in real flight, the portion of atomic oxygen is very small (<< 1 %). In order to account for these factors, the condition in table 2 with a mixture of 96 % nitrogen and 4 % air was used for the wind tunnel tests.

Table 2: Test conditions for L2K experiments

Flow parameter	Value
Total gas mass flow [g/s]	50
Air mass flow [g/s]	2
Nitrogen mass flow [g/s]	48
Total enthalpy [MJ/kg]	6.85
Stagnation pressure [hPa]	89
$h_0 \cdot \sqrt{p_s}$	64.6
Nozzle configuration (throat/exit diameter) [mm]	29/100
Distance from nozzle exit [mm]	120
Test duration [s]	120

The test specimens made of the selected materials consist entirely of solid material. The materials that showed the least degradation were tested three times. Thus, reliability was increased in the testing. The multiple tested materials include I-WBM, TUD-WBM-1 and TUD-WBM-2. The test specimens do not have temperature sensors integrated into the sample structure. The sample geometry used results from the defined fin leading edge geometry. During the tests the test specimens are clamped into a cooled sample holder, which is fixed in the test chamber of the L2K. A water-based cooling system ensures uniform removal of heat from the sample holder during measurements and guarantees firm clamping at the applied thermal loads.

5.2 Test results

Fig. 8 shows the boundary layer that forms around the test specimen. In the upper half of the image, the mechanical surface erosion of the ablation shows the removal of a material particle that is carried away from the test specimen by the free plasma flow.

The test specimen tips of TUD-WBM-2 and oak are shown on the right side Fig. 8. In the case of the TUD-WBM-2 test specimen, the annealing of the test specimen tip and the formation of melt beads from the resins and mineral components contained can be seen. The pointed shape and straight fin leading edge were maintained throughout the test period. The tip of the oak test specimen glows irregularly compared to TUD-WBM-2 and does not form a straight leading edge. The pointed test specimen shape cannot be maintained over the test duration of 120 s. A detachment of porous carbon can be seen on the upper part of the test specimen.
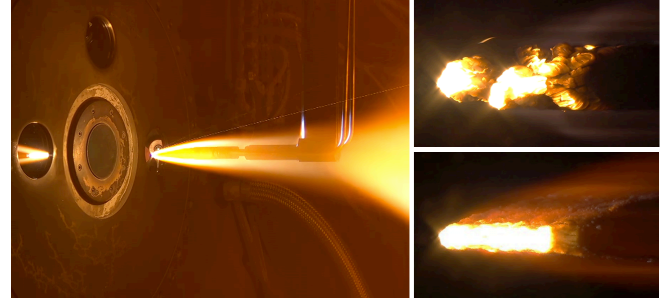

Figure 8: Test specimen during testing (left), test specimen tips of oak (top right) and TUD-WBM-2 (bottom right) at 120 s

The grey background of the temperature measurements of 1- and 2-colour pyrometer in Fig. 9 illustrates the test time of 120 s. At the sample tip of *TUD-WBM-2*, the temperature initially rises from 1500 °C to a maximum of 2300 °C and remains relatively constant over the test duration. In contrast, the temperature measurement of the oak specimen shows clear fluctuations. This is due to a stronger degradation of the material at the test specimen tip, where the focus of the measuring spot of the temperature measurement is lost after flaking of material and is blurred or no longer on the specimen. From t = 20 s onwards, flaking of material can be detected due to strong temperature fluctuations. After 110 s, the 2-colour pyrometer no longer measures any results and drops abruptly from 2400 °C to its starting range of 1000 °C. This is also associated with the loss of the measuring range. This can also be explained by the loss of the measuring spot on the material surface. The two exemplary measurement results of the temperature at the specimen tip clearly show the differences between the specimen materials due to the influence of plasma and high temperature.
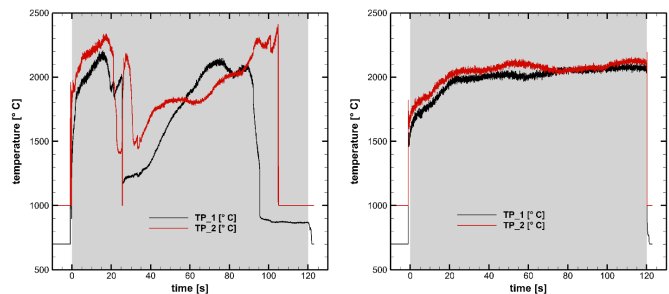

Figure 9: Temperature measurements of an oak (left) and TUD-WBM-2 test specimen

Fig. 10 shows on the left side a test specimen after testing. The thermographic images on the right side of Fig. 10 show the strong thermal load at the test specimen tip, which decreases towards the test specimen holder. The test specimen flanks have lower temperatures than the top and bottom. The TUD-WBM-2 test specimen has a uniform, continuous tip contour after $t = 60$ s as well as $t = 120$ s, while oak has a blunt tip with discontinuous progression.

Figure 10: Test specimen after testing (left), thermographic images of oak (top right) and TUD-WBM-2 (bottom right) at 60 s

6. POST TEST ANALYSIS

The analyses for evaluating the tests in L2K consist of a mass analysis, a cross-sectional area analysis and a contour analysis which are described below.

6.1. Mass analysis

The mass of the test specimens was determined before and after the tests in L2K with a precision balance. For the mass analysis all mass fractions were related to a test time of $t = 120$ s. These are shown together with the results from the preliminary test (highlighted in grey) in Fig. 11, sorted by ascending mass fraction after the test. The calculated densities and information on material densities from the literature or from the manufacturer are also shown.

The wood fibre materials of the test specimens I-WBM, TUD-WBM-1 and TUD-WBM-2 show a lower mass loss of 36 % - 47 % than the solid woods, whose mass losses range between 62 % - 73 %. Compared to the results of the preliminary test, the natural fibre-based materials have a significantly greater mass loss than the composites PTM-1 and PTM-2. TUD-WBM-2 and I-WBM surpass the solid woods tested in the preliminary test with low mass losses. All test specimens of the same material have similar results and therefore validate the material behaviour well. Their results are summarised by their mean value in Fig. 11. The TUD-WBM-2 test specimens are characterised by the lowest mass losses of all tested materials. With an average of 0.89 g/cm³, they have a higher calculated density than the solid woods

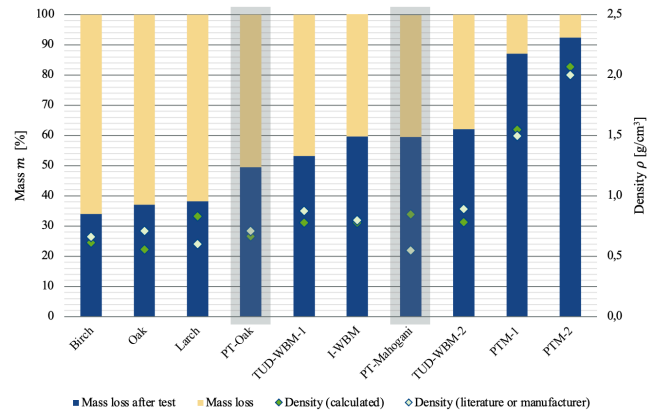oak (0.83 g/cm³) and mahogany (0.85 g/cm³) from the preliminary test. They show up to 4 % less mass loss.

Figure 11: Results of mass analysis

6.2. Cross-sectional area analysis

For the cross-sectional area analysis in the L2K test series the test specimens were cut at a distance of approximately 10 mm from the right sample flank. This distance was chosen because the samples tested in the L2K show a higher and more irregular material loss on the sample flanks. For the further analysis the large test specimen part was considered, since the cutting process damaged material parts of the gate more frequently. During the cutting process, it was found that all wood fibre materials tended to lose less charred material and had a higher structural integrity than the solid woods.

The intact cross-sectional area A_{intact}, the maximum cross-sectional area A_{max}, which results from the intact cross-sectional area and the porous char layer, as well as the original cross-sectional area $A_{original}$ are determined with the program ImageJ. Fig. 12 shows examples of the superimposed results of the cross-sectional area analysis of TUD-WBM-2 and oak compared with the original cross-sectional area $A_{original}$ before the tests in the L2K.
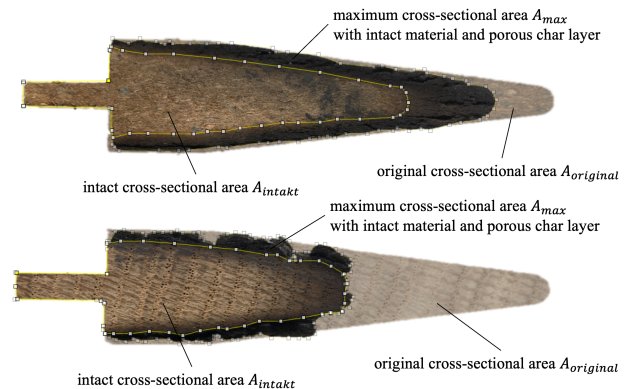

Figure 12: Cross-sectional areas of TUD-WBM-2 (top) and oak (bottom)

The percentage cross-sectional area shares related to t = 120 s are shown for all test specimens sorted by ascending maximum cross-sectional area share in Fig. 13. The results of the preliminary test are highlighted in grey. Analogous to the mass analysis, the calculated densities and information on material densities from the literature or from the manufacturer are shown.

The test specimens made of wood fibre materials show a lower loss of cross-sectional area in the range of 18 % - 38 % than the solid woods, which have a loss of cross-sectional area of 48 % - 65 %. The test specimens made of wood fibre materials have the largest maximum cross-sectional areas of all tested materials after the test. The test specimens of the preliminary test are in line with the cross-sectional ratios of the solid woods. It is noticeable that the wood fibre materials have a larger maximum cross-sectional area, but the intact cross-sectional ratios overlap with the range of the solid woods (28 % - 40 %) with 30 % - 48 %. Especially samples from TUD-WBM-2 show high maximum cross-sectional areas as well as high intact cross-sectional areas, which have a porous, but still structurally intact, carbon layer.
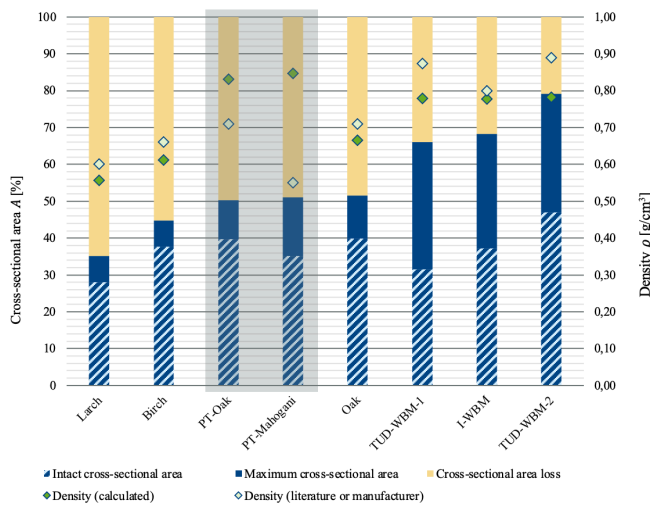

Figure 13: Results of cross-sectional area analysis

6.3. Contour analysis

For the contour analysis, the scans that recorded the contour of the test specimens before and after the test were evaluated and compared with each other. As Fig. 14 shows, the test specimens were scanned in a scan holder with an angle of attack of 35°. Since the samples in the L2K are symmetrically exposed to the plasma flow, only the upper side of the samples, which represents the white part of the sample in Fig. 14, can be used as an example for the contour analysis. To determine a surface contour, the samples were virtually cut along an analysis line, preferably in the centre of the specimen. In this way, a representative cut was made through

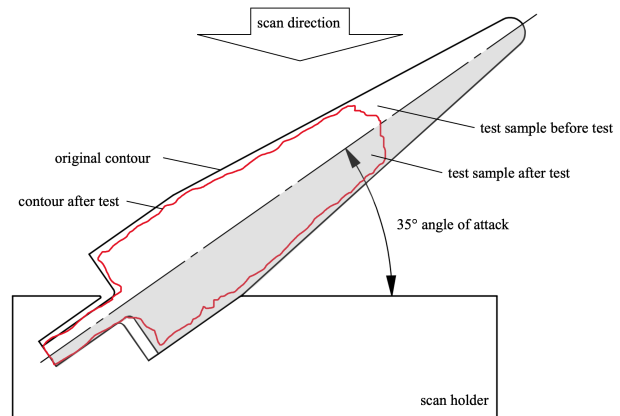the sample, which lies in the area of greatest stress on the test specimen.

Figure 14: Scan of the surface contour of a test specimen

The contours of the upper surfaces of the test specimens Oak, TUD-WBM-1 and TUD-WBM-2 can be seen in Fig. 15 and can be interpreted in the same way as in Fig. 14. The original contour of the top side of the test specimen before the test is marked in black, while the surface contour after the test is marked in red. To the right of the contour curves, the top surfaces of the test specimens are shown with the analysis lines before and after the tests.
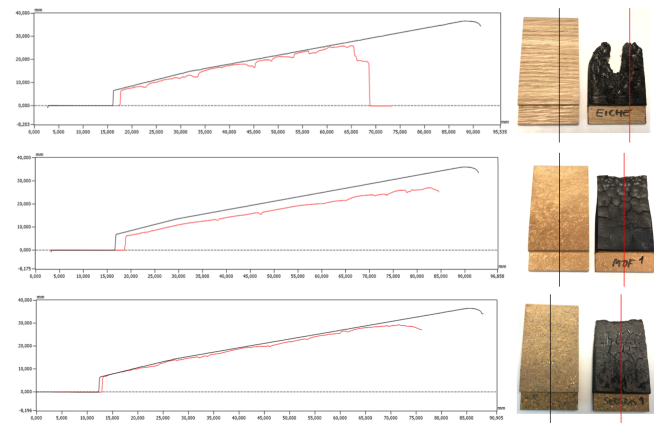

Figure 15: Scan of the surface contour of a test specimen

In the case of the test specimen with oak, a strong loss of material can be seen at the top of the test specimen, as the red contour line on the right-hand side drops steeply downwards. This means that the scanner no longer saw the top of the specimen but the reference surface. Compared to the black contour, the red contour runs relatively close to it. Some indentations can be seen, which can be explained by the porous carbon layer and the formation of a cracked surface. The test specimen of the solid woods show a similar contour as the test specimen from oak. A smaller loss of material can

be seen in the test specimens from TUD-WBM-1 at the tip of the sample. Compared to the black contour line of the sample before the test, the sample has shrunk slightly in the thickness direction, as the red and black contours have a gap. The test specimen from TUD-WBM-2 show a loss of material at the tip of the sample, but the contour of the surface remains well preserved and dimensionally stable after the tests in the L2K, so that the red and black contours do not have a significant distance. Small indentations due to cracks on the surface and curvatures due to melt beads are visible in the contour.

6.4. Results and discussion

In summary, it is evident from the results of the mass and cross-sectional area analysis through the correlation of the mass after the tests and the maximum or intact cross-sectional area with the material density that the bulk density is a significant influencing factor for the resistance of the wood fibre material to thermal loads.

The tested wood fibre materials have a lower mass loss of 36 % - 47 % than solid wood (62 % - 73 %). Likewise, the cross-sectional area loss of the wood fibre materials with 18 % - 38 % is lower than that of the solid woods and cork with 48 % - 65 %. It was observed that the wood fibre samples have larger maximum cross-sectional areas after the test and therefore have a thicker porous carbon layer and pyrolysis zone. However, the intact cross-sectional ratios of the wood fibre materials (30 % - 48 %) overlap with those of the solid woods (28 % - 40 %). All tested specimens show a loss of material at the specimen tip and a shrinkage of their geometry. The specimens of TUD-WBM-2 retain the surface contour the most in comparison with all contour courses and show the smallest changes in the specimen geometry as well as the lowest material loss. The solid woods show the biggest differences from the original contour.

Compared to the glass fibre-based comparative material 1 with a density of 2.0 g/cm^3 previously used by DLR, all tested fin leading edge material variants cannot yet meet the requirements for dimensional stability and geometry retention. In particular, the test specimens of TUD-WBM-2 are characterised by the lowest mass and cross-sectional area loss of all tested materials. They have the highest structural integrity of the porous carbon layer. They also have the best results of the contour analysis and, apart from the material loss at the specimen tip, show good dimensional stability and surface contour. The TUD-WBM-2 material with a density of 0.89 g/cm^3 could contribute to significant mass savings.

7. CONCLUSION

From the analyses and tests, it is evident that untreated wood is not an option for use in fin leading edges of a sounding rocket. Thermal degradation is high and would jeopardise the success of the mission for a component that is part of a critical primary structure assembly.

In contrast, wood fibre materials, which are characterised by higher homogeneity and to which flame retardants have been added, seem to be promising. Compared to solid woods, they have a higher geometry and integrity retention as well as good thermal resistance and high dimensional stability. A fanning of the leading edge could not be detected in the tests in the L2K. The wood fibre material TUD-WBM-2 seems to be particularly promising. In addition to the additive flame retardant, it could be determined by material analyses that the special natural fibre material acts as a reactive flame retardant due to a high salt content and residual components such as sand and suspended matter and delays thermal decomposition.

All wood fibre materials have low thermal conductivities and high specific thermal capacities, which reduce the transport of heat into the fin structure. Due to their production, there is a preferential direction of the fibres in the main plane of the board, which results in a significantly lower heat conductivity in the normal direction compared to in-plane conductivity. The high carbon content of the materials leads to a good ablative thermal protection effect. Compared to the materials used so far by DLR (comparative materials 1 and 2), the wood fibre materials have lower bulk densities and thus lower masses. These properties can result in a mass reduction of the rocket structure and a cost saving potential for the mission.

In summary, it can be concluded that none of the investigated material variants completely fulfils the requirements, but the wood fibre material TUD-WBM-2 can be optimised on the basis of further material analyses and thus represent the innovation potential of sustainable spaceflight materials.

Detailed investigations of the mechanical material behaviour as well as the coupling of flow behaviour, dynamic structure and thermal influences can be carried out in further research. An adaptation of the geometry of the leading edge is thereby considered in order to shift the stagnation point to distribute the thermal load over a larger area.

8. REFERENCES

[1] Institute for Occupational Safety and Health of the German Social Accident Insurance, "GESTIS Substance Database - Sodium chloride (NaCl)", *IFA - Institute for Occupational Safety and Health of the German Social Accident Insurance*, 2022.

[2] G. Oborskyi, I. Pavlenko, J. Trojanowska, V. Ivanov and V. Tonkonogyi, *Advanced Manufacturing Processes III - Selected Papers from the 3rd Grabchenko's International Conference on Advanced Manufacturing Processes (InterPartner-2021),* Springer International Publishing, Odessa/ Schweiz, September 2021.

[3] DIN Deutsches Institut für Normung e.V., "DIN 68364:2003-05: Kennwerte von Holzarten (Rohdichte, Elastizitätsmodul und Festigkeiten)", *Beuth Verlag GmbH*, no. 05, Berlin, pp. 3f, 2003.

[4] P. Niemz, "Untersuchungen zur Wärmeleitfähigkeit ausgewählter einheimischer und fremdländischer Holzarten", *Bauphysik*, Ernst & Sohn Verlag für Architektur und technische Wissenschaften GmbH & Co. KG, Berlin, vol. 29, no. 4, pp. 311-312, 2007.

[5] DIN Deutsches Institut für Normung e.V., "DIN EN ISO 10456: Baustoffe und Bauprodukte - Wärme- und feuchtetechnische Eigenschaften - Tabellierte Bemessungswerte und Verfahren zur Bestimmung der wärmeschutztechnischen Nenn- und Bemessungs-werte (ISO 10456:2007 + Cor. 1:2009); Deutsche Fassung EN ISO 10456:2007 + AC:2009", *Beuth Verlag GmbH*, Berlin, 2010.

[6] DIN Deutsches Institut für Normung e.V., "DIN 68364:2003-05: Kennwerte von Holzarten (Rohdichte, Elastizitätsmodul und Festigkeiten)", *Beuth Verlag GmbH*, Berlin, pp. 3f., 2003.

[7] A. Gülhan und B. Esser, "Arc-Heated Facilities as a Tool to Study Aerothermodynamics Problems of Reentry Vehicles", *Advanced Hypersonic Test Facilities, Progress in Astronautics and Aeronautics*, Bd. 198, Renton, VA, USA, AIAA, pp. 375-403, 2002.

[8] A. Gülhan, B. Esser, U. Koch und K. Hannemann, "Mars Entry Simulation in the Arc Heated Facility L2K", *4th European Symposium on Aerothermodynamics of Space Vehicles*, Capua, Italy, 2002.

[9] A. Gülhan, B. Esser und U. Koch, "Experimental Investigation of Reentry Vehicle Aerothermodynamic Problems in Arc-Heated Facilities", *Journal of Spacecraft and Rockets,* Bd. 38, Nr. 2, pp. 199-206, March-April 2001.